Progress In Electromagnetics Research M, Vol. 95, 165–176, 2020

Pentagonal Shaped UWB Antenna Loaded with Slot and EBG Structure for Dual Band Notched Response

Ameya A. Kadam and Amit A. Deshmukh*

Abstract—In this paper, a planar, compact, and low cost printed microstrip line fed pentagon-shaped ultra-wideband antenna offering dual band notched characteristics response is proposed and investigated. By introducing modified V-shaped slots in the pentagonal patch and hexagonal electromagnetic band gap structures near the feedline, dual band notched response can be realized. The proposed antenna is successfully simulated, designed, and fabricated on an FR-4 substrate. The measured results show that the proposed antenna having dimensions of $35 \times 33 \times 1.6\,\text{mm}^3$ has a bandwidth over the frequency band 2.7–10.6 GHz with magnitude of $S_{11} \leq -10\,\text{dB}$ (VSWR ≤ 2), except 3.7–4.6 GHz (C-band Satellite Communication) and 5.16–6.08 GHz (WLAN) frequency bands. The presented antennas show small group delay variation, nearly omnidirectional radiation pattern and stable gain at working frequencies. Satisfactory results have been obtained in frequency and time-domain analysis of the proposed antenna. The formulation of the center frequency of dual notched frequency band is also proposed.

1. INTRODUCTION

Ultra-wideband (UWB) wireless communication technology has been receiving wide impetus from both academy and industry since the Federal Communication Commission (FCC) unlicensed the frequency band from 3.1 to 10.6 GHz for commercial communication applications in 2002 [1]. Due to the rapid progress in wireless and mobile communication systems, the demand for antennas giving bandwidth (BW) in a few tens of GHz is increased, and in such application monopole antennas are used [2, 3]. However, as these structures are not planar, their integration with microwave integrated circuits is cumbersome. Therefore, printed variations of monopole design are favored [2, 5]. The commonly used shapes of radiating patch in UWB patch antennas are rectangular, triangular, circular, arc, sectoral, and their modified variations [3–9]. Over the designated UWB spectrum (3–10.6 GHz), other narrowband services like WiMAX, IEEE 802.16 (3.3–3.7 GHz), C-band satellite communication (3.7–4.2 GHz), WLAN, IEEE 802.11a, HIPERLAN/2 (5.15–5.825 GHz), and ITU (8.02–8.4 GHz band) exist. In some applications, UWB antenna uses filters to suppress these frequency bands. However, the uses of filter increase the complexity and cost of a UWB system. Therefore, it is necessary to realize a UWB antenna with notched frequency bands to minimize the probable interferences between the UWB and narrowband systems.

Numerous designs of antennas have been reported for notch frequency response in UWB spectrum. The conventional methods are cutting a slot(s) of different shapes on the radiating patch [10, 11], attaching stub(s) with radiating patch [12, 13], incorporating a feeder-embedded slotline resonator [14, 15], incorporating slots in the ground plane [16, 17], utilizing split ring resonators (SRRs) [18, 19], or incorporating electromagnetic band gap structure [20, 21]. As per reported literature, the introduction of stubs, slots in patch or ground plane results in notch band characteristics. However, thorough

Received 28 April 2020, Accepted 23 June 2020, Scheduled 23 August 2020
* Corresponding author: Amit A. Deshmukh (amitdeshmukh76@yahoo.com).
The authors are with the EXTC Department, DJSCE, Mumbai, India.

explanation for highlighting the effects of modifications in patch geometry that yields tunable notch response in terms of patch resonant modes is not provided.

In this paper, a novel design of a pentagonal shape UWB antenna embedded with a modified V-shaped slot and hexagon-shaped electromagnetic band gap (EBG) structures, placed near the microstrip feed line is proposed. Initially, a pentagonal shape UWB antenna is studied. For the frequencies from 2.7 to 11 GHz, an input impedance (Z_{in}) response for return loss (S_{11}) < -10 dB is obtained. The surface current distributions in pentagonal structure are studied for carrying out the identification of its resonant modes. Later, using an optimized pentagon-shaped UWB antenna, with a modified V-shaped slot and hexagon-shaped electromagnetic band gap structures, a notch response over the two frequency bands, i.e., at 3.7–4.6 GHz and 5.16–6.08 GHz, is realized. Here the addition of modified V-shaped slots in pentagonal shape antenna changes the resonance frequencies and input impedance (Z_{in}) at TM_{21} mode which results in notch response in C-band. The second band notch response is obtained by placing two shorted hexagonal EBG structures in the vicinity and on either side of the microstrip line feed. In the lower frequency band, tunable band notch characteristics are obtained by changing the length of modified V-shaped slots. In the higher band, the same is realized either by varying the side length of hexagonal EBG structures or by changing the shorting via position on the EBG unit. The return loss of greater than -5 dB is realized ensuring more than 55% of the reflected power over the notch band frequencies. The presented antennas were optimized on a low cost glass epoxy substrate by using Computer Simulation Technology (CST2019), which was followed by the practical measurements. Using the VNA (ZVH-8) made by Rohde and Schwarz, the return loss of antenna till 8 GHz is measured whereas far field radiation patterns and peak gain are measured using spectrum analyzer (FSC-6) and RF source (SMB 100A). The time domain analysis of the proposed antenna is also carried out. The tunable band notch benefits the reduction of interference with simultaneous applications such as Bluetooth, Wi-Fi, and Wi-MAX.

2. PENTAGONAL UWB PATCH ANTENNA

A regular pentagonal shape UWB antenna, as shown in Figures 1(a) and (b), is designed on a low cost FR4 substrate ($h = 1.6$ mm, $\varepsilon_r = 4.3$, and $\tan\delta = 0.02$). The pentagonal patch having side length 's' = 10.5 mm is selected such that its fundamental TM_{11} mode frequency is around 2.7 GHz while lower band edge frequency is around 2.92 GHz. A feed microstrip line having width of 3 mm for 50 Ω impedance, backed by the ground plane having dimensions 'L_g' = 18 mm and 'W_g' = 33 mm, has been selected. The horizontal separation between the patch and ground plane (p) is taken equal to 1 mm, which yields optimum bandwidth. For the frequencies from 2 to 11 GHz, the simulated resonance curve and return loss (S_{11}) plots are shown in Figure 1(c). The average and vector surface current distributions at the first two modes for pentagonal shape printed monopole antenna are shown in Figures 1(d) and (e). In the pentagonal shape antenna, resonant modes are referred to as TM_{11} and TM_{21}, as they resemble the mode distributions present in the circular patch, having the same patch area with radius 'R_c'. Thus, resonance frequency equation of circular patch can be used for the pentagonal patch with some modifications. For formulating the effective radius in the pentagonal patch, resonant length formulation for printed monopole using a circular patch as reported in [31] is referred for the equivalence. The relation between the side length of pentagonal patch 's' and circular patch radius 'R_c' is given using Equation (1). As seen from Figures 1(d) and (e), current vectors originate from the microstrip feed line. To model this effect in the effective patch radius calculation, term '$L_g + p$' is considered in Equation (2). Although modal surface currents are distributed over the complete patch area, in larger contribution they are present more towards the patch perimeter. Hence this contribution in currents is accounted by including factor 'A' in Equation (2). At TM_{11} mode 'A' = 0.98 yields close matching whereas at TM_{21} mode 'A' = 0.96 gives the matching. Further since the effective radius needs to be modeled, the term $R_c\pi/2$ is selected which basically comes from the factor '$2\pi R_c/4$'. Due to the offset ground plane present in printed monopole antenna, effective dielectric constant 'ε_{re}' for the FR4 substrate is taken as 1.15 [2, 4]. Two modal frequencies are calculated using Equation (3), for $k_{nm} = 1.84118$ and 3.05424. The term 'c' in Equation (3) denotes the velocity of light in free space. For validating the proposed formulations, initially the pentagonal shape patch is simulated for different 's', and its resonance curve plots showing TM_{11} and TM_{21} mode frequencies are given in Figure 2(a).

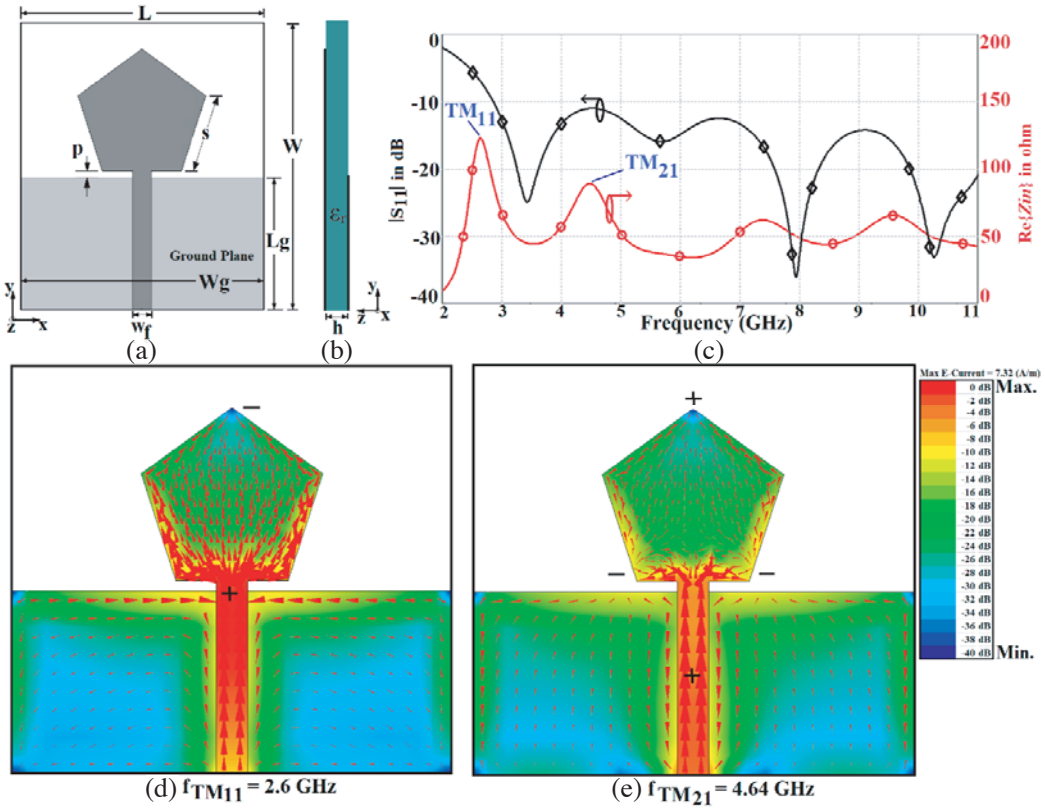

Figure 1. (a) Front and (b) side views of pentagonal shape UWB antenna, its (c) resonance curve and S_{11} plots, and its current distribution plots at (d) f_{TM11} and (e) f_{TM21} modes.

For the same microstrip line feed conditions, the printed circular monopole antenna is simulated using equivalent radius as given in Equation (1), and its resonance curve plots are shown in Figure 2(a). As can be observed, TM_{11} and TM_{21} mode frequencies in two cases are nearly the same which validates Equation (1) for the equivalence. Further to validate Equation (2), for different values of 's', TM_{11} and TM_{21} mode frequencies in pentagon printed monopole antenna are calculated using Equations (2) and (3), and against the simulated values they are plotted in Figures 2(b) and (c). Using the proposed formulation, close prediction of TM_{11} and TM_{21} mode frequencies with % error less than 5% is obtained.

$$R_c = 0.74s \tag{1}$$

$$R_{eq} = \left(A * R_c * \frac{\pi}{2}\right) + p + L_g \tag{2}$$

$$f_{nm} = \frac{k_{nm}.c}{2 * \pi * R_{eq} * \sqrt{\epsilon_{re}}} \tag{3}$$

3. PENTAGONAL SHAPED DUAL BAND NOTCHED UWB ANTENNA

Further novel design of the pentagon-shaped UWB antenna for dual band notch application is presented. Based on the surface current distribution at TM_{21} mode, the position of a modified V-shape slot in pentagonal patch is selected which will perturb its impedance and frequency to realize lower band notch response. Next hexagonal EBG structure is placed near microstrip feed line to help realize higher band notch response, as shown in Figure 3. The effect of a modified V-shaped slot is investigated in detail first by analyzing the resonance curve plot of the antenna in absence of hexagonal EBG structure. The modified V-shaped slot has horizontal slot length as 'L_h' and inclined slot length as 'L_v'. The total slot length is $L_h + 2 * L_v = L_s$. The slot position is selected in such a way that it effectively perturbs the

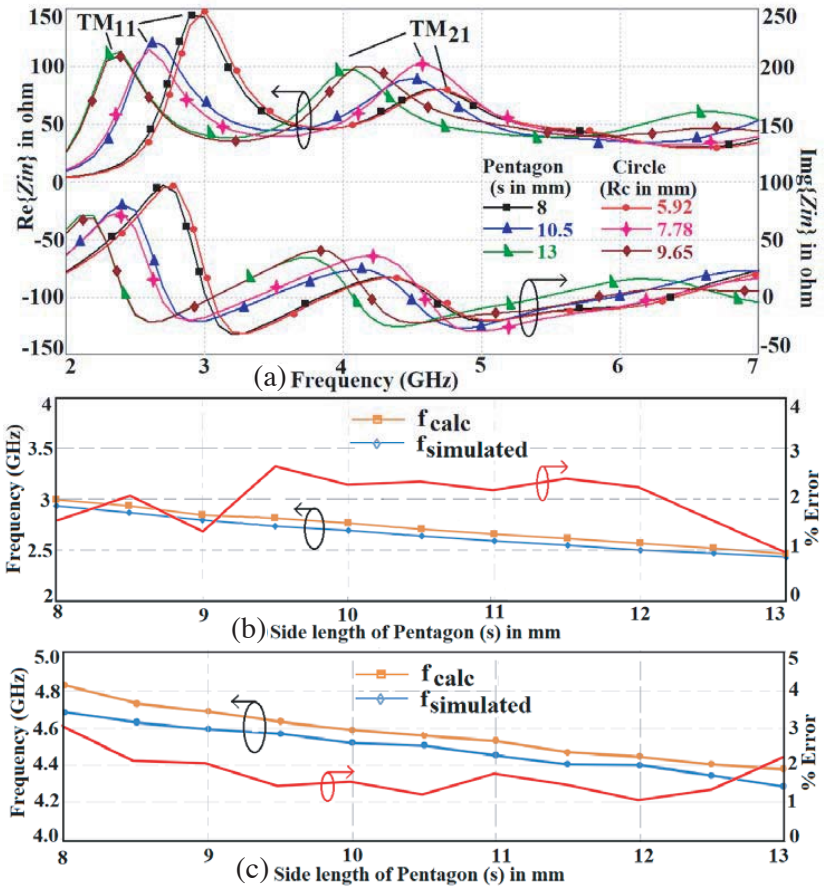

Figure 2. (a) Simulated resonance curve plots for varying patch dimensions in printed pentagon 's' and circular 'R_c' monopole antenna, frequencies and % error plots against variation in 's' at (b) TM_{11} and (c) TM_{21} modes.

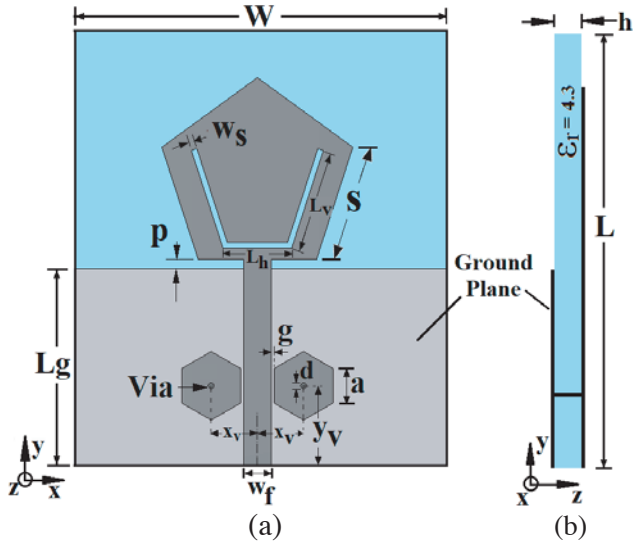

Figure 3. Geometry of dual-band notch UWB antenna (a) front View, (b) side view.

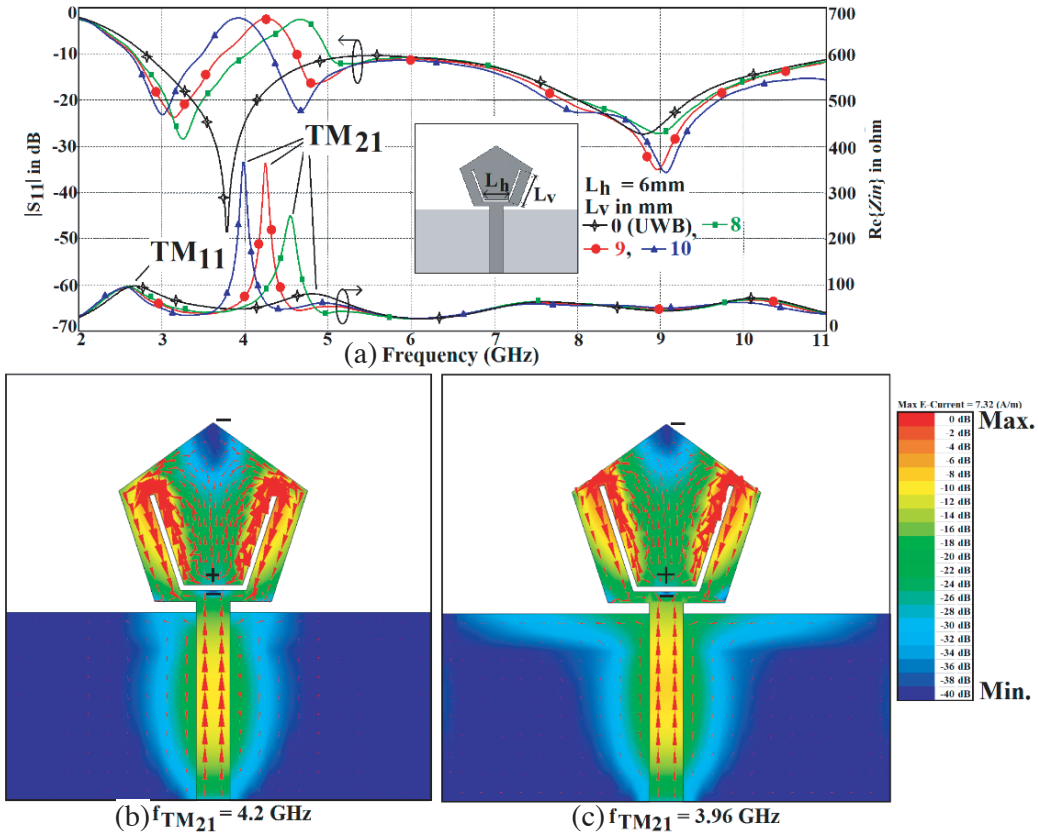

Figure 4. (a) Simulated resonance curve and S_{11} plots for varying inclined slot length L_v, Surface scalar and vector current distribution at TM_{21} frequencies for slot length $L_h = 6\,\text{mm}$, and (b) $L_v = 9\,\text{mm}$, (c) $L_v = 10\,\text{mm}$.

current in the patch present at TM_{21} mode. As the slot dimension is increased, the resonant frequency corresponding to TM_{21} mode gets lowered significantly, and the input impedance at this mode gets increased beyond $200\,\Omega$ resulting in band notch characteristics as seen in Figure 4(a). However, the TM_{11} resonant mode frequency of the patch remains unaltered as currents at it are parallel to modified V-shaped slot. As seen from Figure 4(a), the inclined slot length of 'L_h' = 9 mm which corresponds to 'L_s' = 24 mm, results in simulated return loss greater than $-10\,\text{dB}$ in the frequency band 3.74 to 4.6 GHz. As the inclined slot length L_v is increased to 10 mm which corresponds to 'L_s' = 26 mm, the notch frequency band gets changed to 3.5 to 4.28 GHz. Hence, the tuning of notch band is possible by varying the slot length 'L_v'. The surface current distributions in the antenna for 'L_v' = 9 mm and 10 mm at corresponding resonant frequencies of 4.2 GHz and 3.96 GHz are shown in Figures 4(b) and (c). The density of current is maximum around modified V-shaped slot at the resonant TM_{21} mode frequency.

Further to reduce the interference with WLAN bands, hexagon-shaped EBG structures are placed in the vicinity of a microstrip feed line. The designed and optimized unit cell of EBG structure is shown in Figure 5(a). The unit cell structure is simulated in eigenmode solution of CST2019, and the dispersion diagram based on rectangular (irreducible) Brillouin zone is plotted as shown in Figure 5(b). The unit cell parameters are taken as: substrate dielectric constant 'ε_r' = 4.4, substrate height 'h' = 1.6 mm, hexagonal patch side 'a' = 3 mm, diameter of each via 'd' = 0.5 mm. From the dispersion diagram, we observe that band gap exists for hexagonal shaped EBG structure. The band gap (gray part) is observed between mode-1 and mode-2 centered at $f_c = 5.65\,\text{GHz}$ with lower cutoff frequency $f_l = 5.25\,\text{GHz}$ and higher cutoff frequency $f_h = 6.05\,\text{GHz}$. The geometry of EBG structures and equivalent circuit model designed based on LC resonator to explain the mechanism of the EBG structure coupled to the microstrip

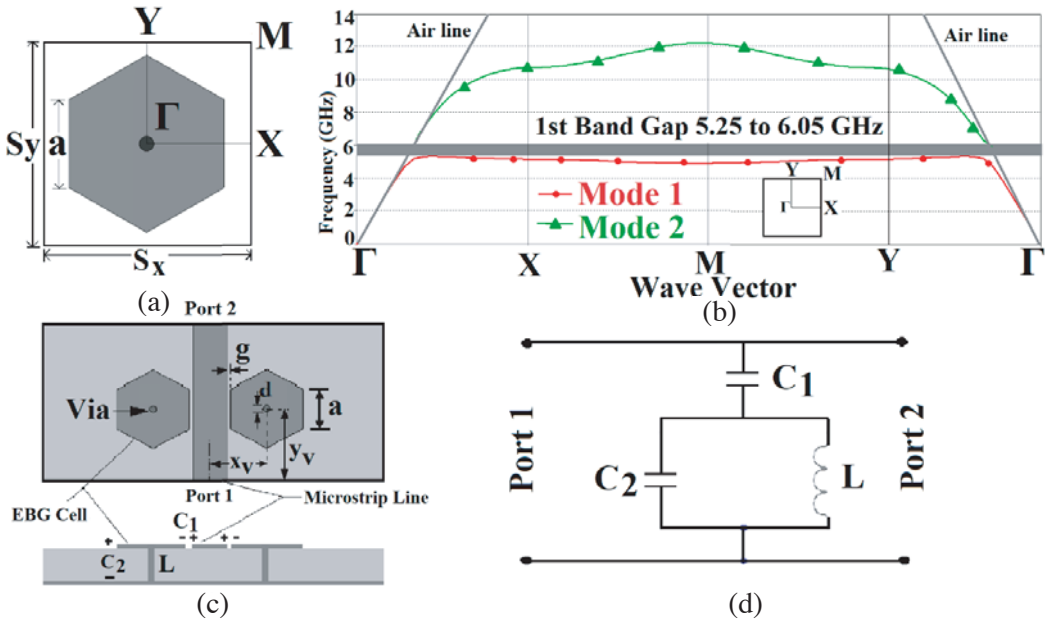

Figure 5. (a) Hexagonal Electromagnetic Band Gap unit cell structure, (b) dispersion diagram for the hexagonal EBG structure, (c) EBG structure used in vicinity of microstrip line and, (d) equivalent resonant circuit of unit EBG cell.

feed line are depicted in Figures 5(c) and (d). Then based on the LC-parameters, the resonant frequency of the EBG cell can be obtained by [30],

$$f_c = \frac{1}{2 * \pi * \sqrt{L\left(C_1 + C_2\right)}} \tag{4}$$

$$L = 2 \times 10^{-7} h \left[\ln\left(\frac{h}{d}\right) + 0.5\left(\frac{d}{h}\right) - 0.75\right] \tag{5}$$

$$C_1 = \frac{w\varepsilon_0\left(1 + \varepsilon_r\right)}{\pi} \cosh^{-1}\left(\frac{w+g}{g}\right) \tag{6}$$

where 'C_1' is the edge capacitance between the EBG patch and microstrip line, and 'C_2' is capacitance between EBG patch and ground plane. For the hexagon-shaped EBG structure, $w = \sqrt{3}a$ is taken into account for the calculation of 'C_1'. The inductance 'L' is due to current flow through the via.

To understand the influence of some important parameters of EBG structure on the notched characteristics, parametric studies are carried out. The effects of variation in the diameter 'd' of shorting via in EBG structure is shown Figure 6(a). It is evident that as the diameter of the via increases, the center frequency of notched band shifts to a higher frequency range with some increase in notched bandwidth. When the diameter of via increases, the inductance related to via decreases which results in the increase in the center frequency of notched band. The increase in the bandwidth is attributed to the decrease in the quality factor. The effect of variation of via location in horizontal and vertical directions on the magnitude of S_{11} is also simulated and investigated. For a fixed horizontal via location 'x_v' = 4.5 mm, the effect of variation along vertical direction (y_v) is plotted in Figure 6(b). As the via locations are moved from the lowermost vertex of hexagonal EBG structure (y_v = 4.25 mm) to the uppermost vertex of EBG structure (y_v = 9.75 mm), the band notch central frequency increases initially up to central location (y_v = 7 mm) and then again decreases. However, it is also observed that except at the central location of via (x_v = 4.5 mm, y_v = 7 mm), the slight impedance mismatch occurs in the frequency range of 6–8.5 GHz. Hence, the optimum vertical position of via is 'y_v' = 7 mm. Further, for a fixed vertical location 'y_v' = 7 mm, the effect of variation along horizontal direction (x_v) is plotted in Figure 6(c). As the via locations are moved horizontally away from the feedline (x_v = 2.2 to 6.8 mm), the band notch center frequency increases initially up to central location (x_v = 4.5 mm) and then again

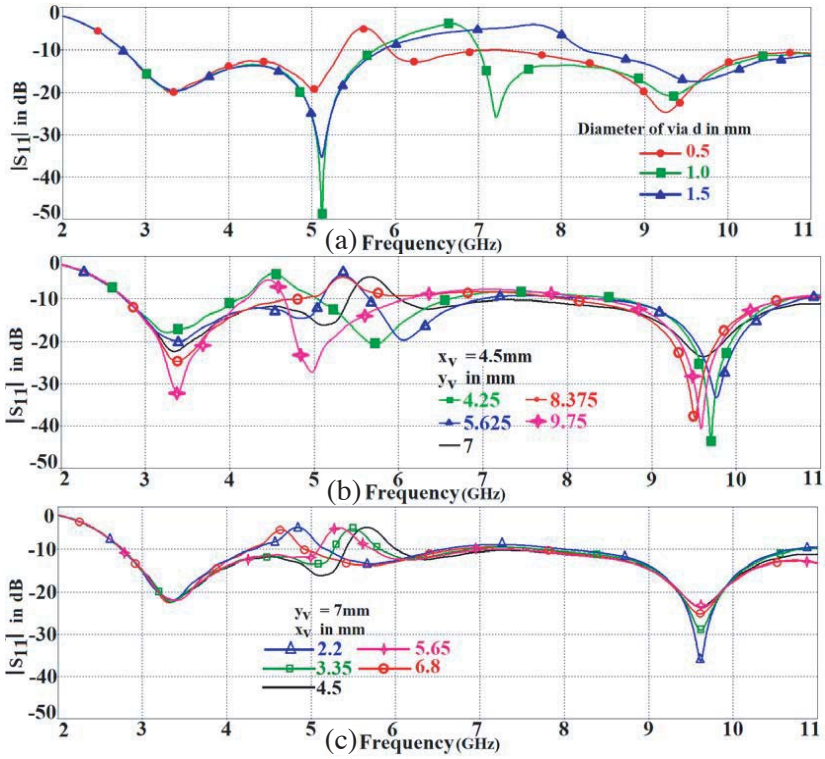

Figure 6. Plot of simulated magnitude of S_{11} for variation in (a) via diameter for fixed location $x_v = 4.5\,\text{mm}$, $y_v = 7\,\text{mm}$, (b) via location y_v for fixed value of $x_v = 4.5\,\text{mm}$, $d = 0.5\,\text{mm}$, (c) via location x_v for fixed value of $y_v = 7\,\text{mm}$, $d = 0.5\,\text{mm}$.

decreases, but the notch bandwidth almost remains constant as seen from Figure 6(c). Based upon above parametric study, to achieve notch frequency response around 4 and 5.5 GHz, a pentagon-shaped dual band notched antenna incorporated with a modified V-shaped slot and hexagonal EBG structure with dimensions as mentioned in Table 1 is fabricated.

Table 1. Optimized parameters for proposed dual band-notched antenna.

Parameter	Size (mm)	Parameter	Size (mm)	Parameter	Size (mm)
L	35	s	10.5	g	0.5
W	33	L_v	9	d	0.5
L_g	18	L_h	6	a	3
w_f	3	w_s	0.5	x_v	4.5
h	1.6	p	1	y_v	7

The plots of the simulated and measured magnitudes of S_{11} till 8 GHz are shown in Figure 7(a), while the fabricated prototype is shown in Figures 7(b) and (c). The measured results show that the proposed antenna has an impedance bandwidth over the frequency band 2.7–10.6 GHz with $|S_{11}| \leq -10\,\text{dB}$, except for the region 3.7–4.6 GHz and 5.16–6.09 GHz where notch response is observed. The measured result is in close agreement with the simulated one.

The gain and far-field radiation patterns of the antennas were measured using the spectrum analyzer (FSC-6) made by Rohde & Schwarz and RF source (SMB 100A) in the minimum reflection surroundings with more than $2D^2/\lambda_0$ distance between standard horn antennas of the corresponding frequencies and

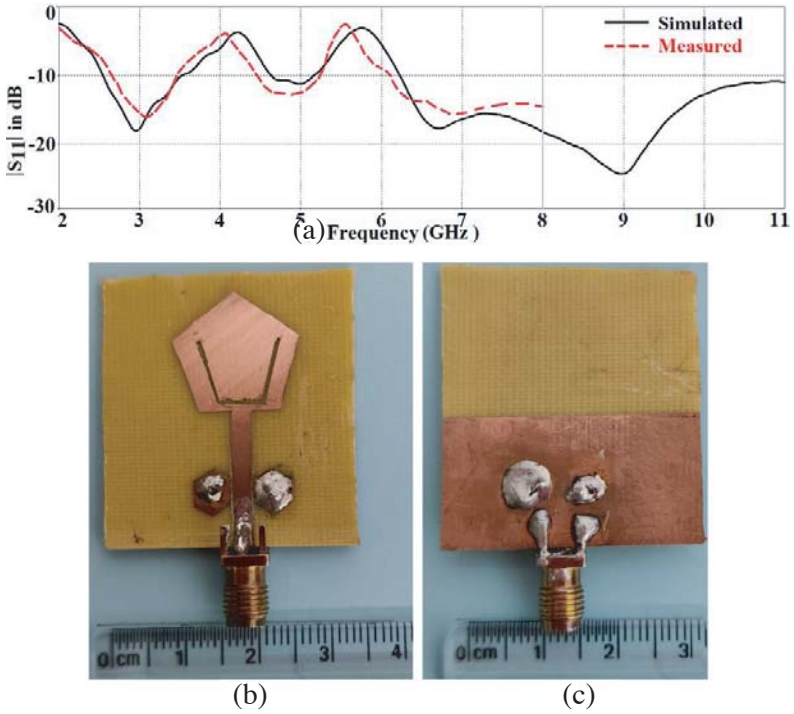

Figure 7. Measured and simulated magnitude of S_{11} plot of proposed antenna, Fabricated prototype of proposed dual-band notched antenna (b) front view, (c) back view.

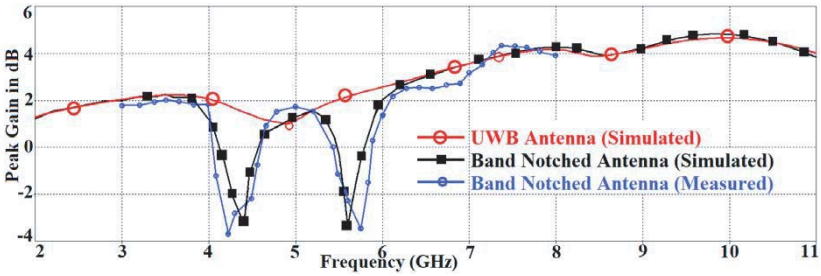

Figure 8. Peak gain plot of pentagonal shaped Dual-band notched UWB antenna.

proposed antenna under test. Here 'D' is taken as the maximum dimension of antenna. The measured gain of proposed antenna till 8 GHz is shown in Figure 8, while the normalized measured radiation patterns at 3.5, 5, and 7.5 GHz in the E- and H-planes are shown in Figure 9. The gain varies between 2 dB and 5 dB over the 2.7–10.6 GHz frequency range except in the 3.7–4.6 GHz and 5.16–6.09 GHz notched frequency bands which demonstrates that band-notched function is good. The antenna exhibits a stable omnidirectional radiation over UWB except in notched frequency bands. At higher frequencies, the radiation pattern deteriorates because of the unequal phase distribution and significant magnitude of higher order modes. Omnidirectional characteristics can be improved by using a thin substrate or a substrate with low dielectric constant. The proposed antenna has nearly omnidirectional radiation characteristic in the H-plane and a figure of eight radiation pattern in the E-plane over the desired band.

The time domain performance of UWB antenna is vital for pulsed communication systems. The group delay is a measure of the time delay of an impulse signal at various frequencies. The measurement of the time domain parameters has been done using Rohde and Schwarz ZVH-8 vector network analyzer in the free space environment. To understand this time domain behavior of the signal at notched

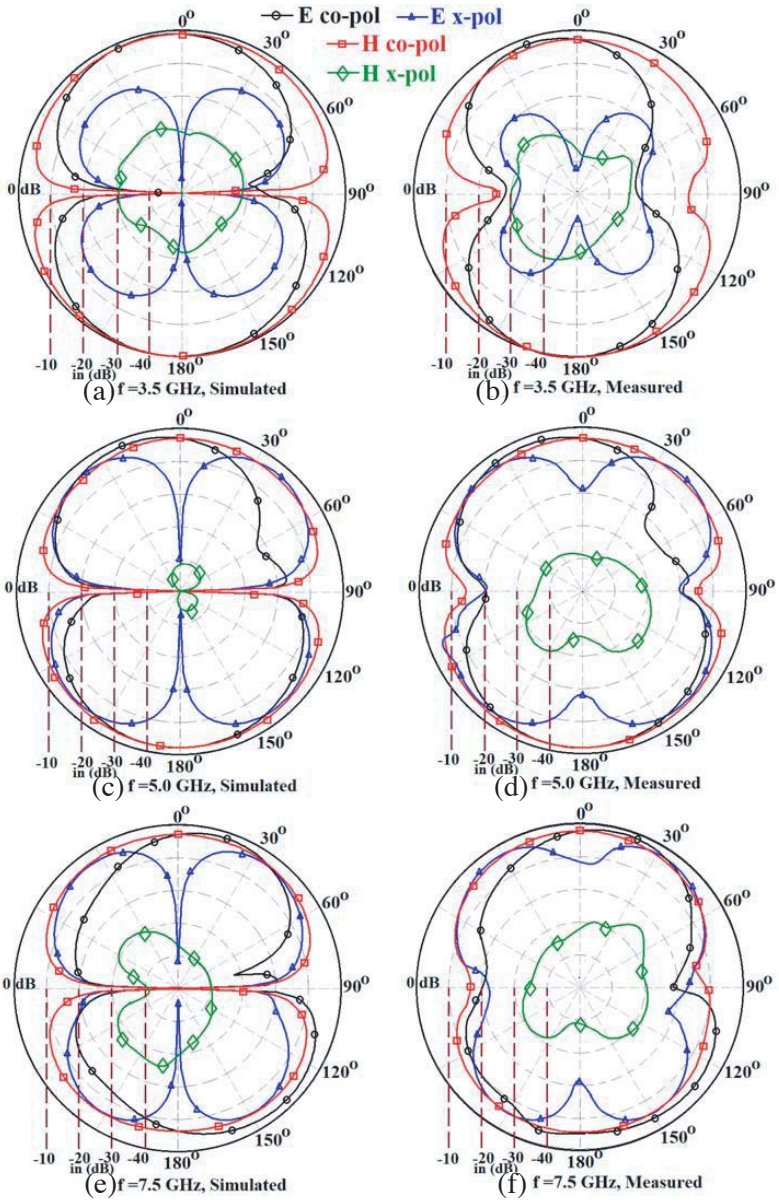

Figure 9. Simulated and measured E-field (yz-plane) and H-field (xz-plane) radiation pattern.

frequencies, two identical antennas are placed in face to face and side by side configurations with a distance of 300 mm. For both configurations, the simulated and measured group delays and magnitudes of S_{21} (transfer function) are shown in Figures 10(a) and (b). It can be seen that high delay is observed at both center frequencies of notched bands (4.2 and 5.8 GHz), whereas apart from these frequencies the simulated and measured relative group delays for the face to face and side to side configurations are almost constant. It is also shown in Figures 10(a) and (b) that the magnitude of S_{21} (transfer function) is less than -50 dB at notched frequencies for both configurations. The time domain analysis of antenna parameters proves that the proposed antenna is a good candidate for dual band-notched UWB applications.

The comparison of antenna size and several notch bands of the proposed antenna with reported single and dual band-notched UWB antennas is shown in Table 2. The notch bands responses are obtained by placing two square EBG structures [21] and slitted EBGs near the feed line in [23]. The band notch response is obtained by incorporating an inverted U-slot in the feed line [22]. The combination of

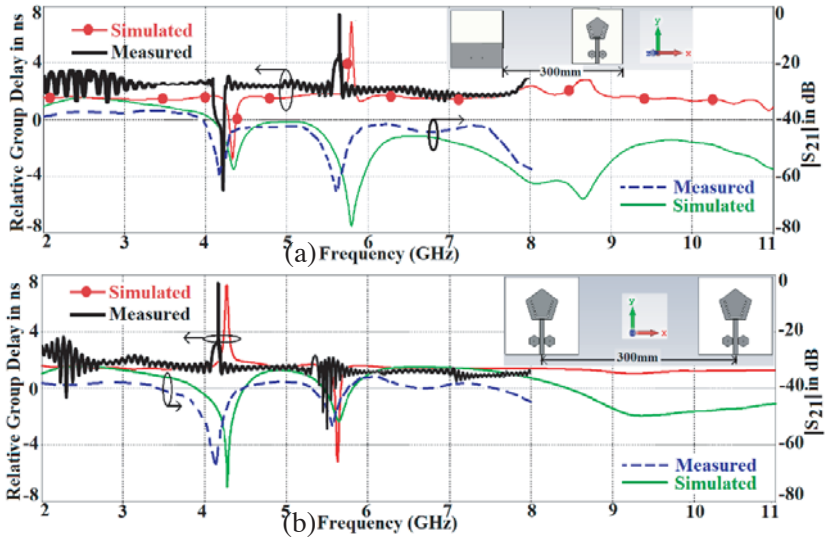

Figure 10. Simulated and measured group delay and magnitude of S_{21} (transfer function) of proposed dual band-notched UWB antenna (a) face to face and (b) side by side configuration.

slots in the patch and SRR structures in the vicinity of the feed line are used to realize dual band-notched responses [24]. A filter with U-shape or L-shape stub structures on the backside of a CPW-fed circular UWB antenna realizes notch-band response, but the presence of multiple vias near each other increases structure complexity [25]. Slots are incorporated in the patch to realize band notch responses, but the use of a dielectric resonator increases the volume of antenna significantly [26]. A rectangular strip is connected to the radiator through vias to realize dual band-notch responses which increases fabrication complexity [27]. In order to attain a single band-notched response in a differential-fed antenna, two pairs of $\lambda/4$ length stubs are introduced in the ground plane [29]. In the reported literature mentioned in Table 2, the designed antennas have a larger dimension or complexity in terms of the fabrication of structures. Also, the earlier published works do not explain the modal analysis of the structure and perturbation of current at particular mode to create impedance mismatch resulting in notch response. The novelty of this work includes detailed modal analysis to realize the notched characteristics in the proposed structure. Also, the proposed antenna has a compact volume of 1155 mm^2 and is capable of producing two notch bands.

Table 2. Comparison with reported single and dual-band notched UWB antennas.

Reference	Antenna size (mm^2) $L \times W$	Number of Notch bands	Frequency Range (GHz)
[21]	$52 \times 32 = 1664$	2	3.11–10.6
[22]	$30 \times 40 = 1200$	2	2.8–11
[23]	$34 \times 34 = 1156$	1	3.1–10.6
[24]	$78 \times 44.6 = 3478$	2	2.63–10.86
[25]	$60 \times 60 = 3600$	1	2.8–9.0
[26]	$50 \times 40 = 2000$	2	2.9–10.8
[27]	$40 \times 43 = 1720$	2	2.9–11
[28]	$40 \times 30 = 1200$	2	2.55–11
[29]	$35 \times 30 = 1050$	1	3.1–12
Proposed Work	$35 \times 33 = 1155$	2	2.7–11

4. CONCLUSIONS

A UWB pentagonal shape antenna is proposed, which yields BW from 2.7 GHz to more than 10.6 GHz. Further by altering UWB antenna design, tunable notch responses are obtained by using modified V-shaped slots and hexagon-shaped EBG structures in 3.7–4.6 GHz and 5.16-6.08 GHz frequency bands, respectively. The surface current distributions at the notched frequency with and without modified V-shaped slot are also computed and investigated. The slot dimension increases the input impedance of TM_{21} mode and decreases the resonance frequency which results in notch characteristics. The experimentally measured results have shown a satisfactory agreement with the simulated ones. The developed antenna provides good radiation patterns in both E- and H-planes over UWB range except in the notched band. The antenna also provides linear transfer function and minimal group delay variation except in the notched band.

REFERENCES

1. First Report and Order, "Revision of part 15 of the commission's rules regarding ultra-wideband transmission systems," Federal Communications Commission, FCC 02-48, 2002.
2. Kumar G. and K. P. Ray, *Broadband Microstrip Antenna*, Artech House, USA, 2003.
3. Garg, B. P., I. Bahl, and A. Ittipiboon, *Microstrip Antenna Design Handbook*, Artech House, USA, 2001.
4. Ray, K. P., "Design aspects of printed monopole antennas for ultra-wide band applications," *Int. J. Antennas Propag.*, Vol. 2008, 1–8, 2008.
5. Agrawall, N. P., G. Kumar, and K. P. Ray, "Wide-band planar monopole antennas," *IEEE Trans. Antennas Propag.*, Vol. 46, No. 2, 294–295, 1998.
6. Wong, K. L. and Y. F. Lin, "Stripline-fed printed triangular monopole," *Electron. Lett.*, Vol. 33, No. 17, 1428–1429, 1997.
7. Jose, J. V., A. S. Rekh, and M. J. Jose, "Double-elliptical shaped miniaturized micro strip patch antenna for ultra-wide band applications," *Progress In Electromagnetics Research C*, Vol. 97, 95–107, 2019.
8. Ray, K. P., S. S. Thakur, and R. A. Deshmukh, "UWB printed sectoral monopole antenna with dual polarization," *Microw. Opt. Technol. Lett.*, Vol. 54, No. 9, 2066–2070, 2012.
9. Thomas, P., D. D. Krishna, M. Gopikrishna, U. G. Kalappura, and C. K. Aanandan, "Compact planar ultra-wideband bevelled monopole for portable UWB systems," *Electron. Lett.*, Vol. 47, No. 20, 1112–1114, 2011.
10. Mewara, H. S., J. K. Deegwal, and M. M. Sharma, "A slot resonators based quintuple band-notched Y-shaped planar monopole ultra-wideband antenna," *AEU — Int. J. Electron. Commun.*, Vol. 83, 470–478, 2018.
11. Zhu, Y., F.-S. Zhang, C. Lin, Q. Zhang, and J.-X. Huang, "A novel dual band-notched monopole antenna for ultra-wideband application," *Progress In Electromagnetics Research Letters*, Vol. 16, 109–117, 2010.
12. Deshmukh, A. A. and P. V. Mohadikar, "Modified rectangular shape patch antennas for ultra-wide band and notch characteristics response," *Microw. Opt. Technol. Lett.*, Vol. 59, No. 7, 1524–1529, 2017.
13. Guichi, F., M. Challal, and T. A. Denidni, "A novel dual band-notch ultra-wideband monopole antenna using parasitic stubs and slot," *Microw. Opt. Technol. Lett.*, Vol. 60, No. 7, 1737–1744, 2018.
14. Haraz Ahmed, O. M. and A. R. Sebak, "Numerical and experimental investigation of a novel ultrawideband butterfly shaped printed monopole antenna with bandstop function," *Progress In Electromagnetics Research C*, Vol. 18, 111–121, 2011.
15. Abbosh, A. M., "Design of a CPW-fed band-notched UWB antenna using a feeder-embedded slotline resonator," *Int. J. Antennas Propag.*, Vol. 2008, 1–5, 2008.

16. Wang, C., Z.-H. Yan, B. Li, and P. Xu, "A dual band-notched UWB printed antenna with C-shaped and U-shaped slots," *Microw. Opt. Technol. Lett.*, Vol. 54, No. 6, 1450–1452, 2012.
17. Mishra, S. K. and J. Mukherjee, "Compact printed dual band-notched U-shape UWB antenna," *Progress In Electromagnetics Research C*, Vol. 27, 169–181, 2012.
18. Yadav, A., S. Agrawal, and R. P. Yadav, "SRR and S-shape slot loaded triple band notched UWB antenna," *AEU — Int. J. Electron. Commun.*, Vol. 79, 192–198, 2017.
19. Lv, Y., J. Zhang, and H. Hou, "A novel triple band-notched UWB printed monopole antenna," *Progress In Electromagnetics Research M*, Vol. 81, 85–95, 2019.
20. Jaglan, N., B. K. Kanaujia, S. D. Gupta, and S. Srivastava, "Triple band notched UWB antenna design using electromagnetic band gap structures," *Progress In Electromagnetics Research C*, Vol. 66, 139–147, 2016.
21. Mandal, T. and S. Das, "Design of dual notch band UWB printed monopole antenna using electromagnetic-bandgap structure," *Microw. Opt. Technol. Lett.*, Vol. 56, No. 9, 2195–2199, 2014.
22. Choukiker, Y. K. and S. K. Behera, "Modified Sierpinski square fractal antenna covering ultra-wide band application with band notch characteristics," *IET Microwaves, Antennas Propag.*, Vol. 8, No. 7, 506–512, 2014.
23. Ghahremani, M., C. Ghobadi, J. Nourinia, M. S. Ellis, F. Alizadeh, and B. Mohammadi, "Miniaturised UWB antenna with dual-band rejection of WLAN/WiMAX using slitted EBG structure," *IET Microwaves, Antennas Propag.*, Vol. 13, No. 3, 360–366, 2019.
24. Tsai, L. C., "A ultrawideband antenna with dual-band band-notch filters," *Microw. Opt. Technol. Lett.*, Vol. 59, No. 8, 1861–1866, 2017.
25. Mansouri, Z., F. B. Zarrabi, and A. Saee Arezoomand, "Multi notch-band CPW-fed circular-disk UWB antenna using underground filter," *Int. J. Electron. Lett.*, Vol. 6, No. 2, 204–213, 2018.
26. Denidni, T. A. and Z. Weng, "Hybrid ultrawideband dielectric resonator antenna and band-notched designs," *IET Microwaves, Antennas Propag.*, Vol. 5, No. 4, 450–458, 2011.
27. Zhu, F., et al., "Dual band-notched tapered slot antenna using $\lambda/4$ band-stop filters," *IET Microwaves, Antennas Propag.*, Vol. 6, No. 15, 1665–1673, 2012.
28. Fertas, K., F. Ghanem, A. Azrar, and R. Aksas, "UWB antenna with sweeping dual notch based on metamaterial SRR fictive rotation," *Microw. Opt. Technol. Lett.*, Vol. 62, No. 2, 956–963, 2020.
29. Zhang, J., T. Chen, L. Hua, and W. Wang, "A compact differential-fed UWB antenna with band-notched characteristics," *Progress In Electromagnetics Research M*, Vol. 83, 171–179, 2019.
30. Yang, F. and Y. Rahmat-Samii, "Microstrip antennas integrated with electromagnetic band-gap (EBG) structures: A low mutual coupling design for array applications," *IEEE Trans. Antennas Propag.*, Vol. 51, No. 10 II, 2936–2946, 2003.
31. Deshmukh, A. A., P. Mohadikar, and S. Pawar, "Formulation of resonant length for regular and modified shapes printed monopole antennas," *Int. J. Microw. Opt. Technol.*, Vol. 13, No. 6, 478–486, 2018.